



CHORUS

This is the accepted manuscript made available via CHORUS. The article has been published as:

Density functional plus dynamical mean-field theory of the spin-crossover molecule $\text{Fe}(\text{phen})_2(\text{NCS})_2$

Jia Chen, Andrew J. Millis, and Chris A. Marianetti

Phys. Rev. B **91**, 241111 — Published 19 June 2015

DOI: [10.1103/PhysRevB.91.241111](https://doi.org/10.1103/PhysRevB.91.241111)

Density Functional plus Dynamical Mean-Field Theory of the Spin-Crossover Molecule $\text{Fe}(\text{phen})_2(\text{NCS})_2$

Jia Chen^{1,2}, Andrew J. Millis², Chris A. Marianetti¹

¹*Department of Applied Physics and Applied Mathematics,
Columbia University, New York, New York 10027, USA and*

²*Department of Physics, Columbia University, New York, New York 10027, USA*

We study the spin-crossover molecule $\text{Fe}(\text{phen})_2(\text{NCS})_2$ using density functional theory (DFT) plus dynamical mean-field theory, which allows access to observables not attainable with traditional quantum chemical or electronic structure methods. The temperature dependent magnetic susceptibility, electron addition and removal spectra, and total energies are calculated and compared to experiment. We demonstrate that the proper quantitative energy difference between the high-spin and low-spin state, as well as reasonably accurate values of the magnetic susceptibility can be obtained when using reasonable interaction parameters. Comparisons to DFT and DFT+U calculations demonstrate that dynamical correlations are critical to the energetics of the low-spin state. Additionally, we elucidate the differences between DFT+U and spin density functional theory (SDFT) plus U methodologies, demonstrating that DFT+U can recover SDFT+U results for an appropriately chosen on-site exchange interaction.

The combination of density functional theory (DFT) and dynamical mean-field theory (DMFT) is now established in condensed matter physics as a successful theory of materials with strong local electron correlations.^{1,2} Initially devised as a theory of extended (infinite) systems, the method has been extended to finite systems³⁻⁹ and has been used to demonstrate that many-body effects are important for ligand binding on the active center of protein myoglobin and haemoglobin.^{10,11} As compared to traditional highly accurate quantum chemical methods DFT+DMFT provides many advantages including excited-state properties, nonzero temperatures and treatment of arbitrary strength of local correlations. Also, because the computational cost scales linearly with the number of symmetry-inequivalent correlated atoms, the method can be used to treat molecules containing many transition metal or actinide atoms. However, its broad applicability and quantitative effectiveness in the quantum chemical context is not yet fully established.

Here we apply the DFT+DMFT method to study spin-crossover complexes: molecular species that change spin state upon increase of temperature or other changes in environment. Spin crossover molecules provide an important challenge to theory, requiring both accurate energetics and the ability to treat excitations in a situation that (because of the spin) necessarily involves strong electron correlations. Insights gained from study of spin crossover materials could potentially be useful for the design of thin films^{12,13} or single-molecule¹⁴ spintronic devices.

This paper provides a comprehensive DFT+DMFT description of $\text{Fe}(\text{phen})_2(\text{NCS})_2$,¹⁵ (structure shown in panel (b) of Fig. 3) a member of an extensively studied and still expanding family of spin-crossover complexes based on $\text{Fe}(\text{II})$.^{16,17} We compute the magnetic susceptibility, electron addition and removal spectra, and total energy, finding results in good agreement with experimental data when using reasonable interaction parameters. Our analysis enables us to infer that the metal-to-ligand bond length is the control parameter

of spin transition. We explore the sensitivity of various observables to the double-counting correction and the on-site interactions U and J , demonstrating that $\text{Fe}(\text{phen})_2(\text{NCS})_2$ is a useful testbed for current and future first-principles methods. Comparison of our results to those obtained with the Hartree approximation (ie. DFT+U^{18,19}), demonstrates the importance of dynamical fluctuations in capturing the physics of strong hybridization that is present in the LS state.

The key feature of $\text{Fe}(\text{phen})_2(\text{NCS})_2$ is the octahedrally coordinated $\text{Fe}(\text{II})$ ion.^{16,17} As the temperature is increased above $T^* = 176\text{K}$, there is an abrupt increase in magnetic susceptibility which is believed to be related to a change in the electronic configuration from the nominal low-spin (LS) state $t_{2g}^6 e_g^0$ with no unpaired electrons to the nominal high spin (HS) state $t_{2g}^4 e_g^2$ with 4 unpaired electrons. The average Fe-to-N distance, $d(\text{Fe} - \text{N})$, is also longer by about 0.2\AA in the HS than in the LS state.²⁰ Experimental measurements estimate that the energy splitting between LS and HS states is $E_{\text{HS}} - E_{\text{LS}} \approx 0.13\text{eV}$.²¹ This difference is much greater than the contribution $k_B T \cdot \ln 5 \approx 0.025\text{eV}$ to the free energy from the change in electronic entropy.

Obtaining a LS-HS energy difference of the correct order of magnitude has proven challenging for theory. Spin density functional theory in the generalized gradient approximation (GGA) level overestimates the stability of low-spin state while Hartree-Fock theory incorrectly predicts HS as the ground state.²¹ These considerations motivated people to consider hybrid functionals, which interpolate between DFT and HF energies and therefore can be tuned to obtain the desired energy difference. However, the amount of exact exchange was found to be less than is normally considered reasonable.^{21,22} An extensive study of spin-crossover molecules using modern density functional theory, including meta-GGA and hybrid meta-GGA and double-hybrid functional, shows, generally speaking, relative energies of spin multiplici-

ties are still challenging for DFT methods.²³ The spin density functional plus U (SDFT+U)^{19,24} method was also applied to this system, but again obtaining the correct energy splitting required choosing $U \approx 2.5eV$, much smaller than is believed to be relevant for Fe.^{25,26} Diffusion Quantum Monte-Carlo method has also been applied to charged spin-crossover molecules, although direct comparisons to experiments are not currently feasible for charged systems.^{27,28} Very recently a detailed quantum chemical calculation based on CASPT2 methods reported an energy splitting of 0.17eV,²⁹ indicating the importance of correlations in this system.

Here we perform fully charge self-consistent DFT+DMFT calculations of the total energy using the method described in Ref. 30 and 31. The DFT part of our calculations use the Vienna ab initio simulation package (VASP),^{32,33} with the Perdue-Burke-Ernzerhof exchange-correlation functional,³⁴ an energy cutoff of 400eV and a supercell of edge length 15Å. Maximally-localized Wannier functions (MLWF),³⁵ constructed using an energy window of 26.5eV with 4.4eV of empty states (120 states total), were used to represent the so-called hybridization window and to construct the correlated subspace^{30,31} in which DMFT is performed. The hybridization window includes all 85 occupied states as well as the anti-bonding π orbitals on phenanthroline and thiocyanate groups that hybridize with the t_{2g} orbitals of Fe. The correlated subspace is chosen as the five d -like iron-centered orbitals. Following common practice, for the intra- d interaction we take the density-density part of the full on-site Coulomb interaction, parametrized by two independent interaction constants denoted as U and J (we use the form stated in Ref. 36) with (unless otherwise specified) $U=5.0$ eV and $J=0.85$ eV, consistent with estimates in the literature for Fe in various compounds.^{10,11,37,38} A double counting term is needed to remove the on-site d interactions present in the Hartree and exchange-correlation functionals. We use the spin-independent form of Anisimov¹⁹

$$V_{dc} = U'(N_d - \frac{1}{2}) - J(\frac{N_d}{2} - \frac{1}{2}) \quad (1)$$

Park et al,^{30,31} noted that one should allow for the possibility that the coefficient U' in Eq. 5 differs from the coefficient U in the interaction. However in this paper we set $U = U'$ everywhere except in the discussion of Fig. 4.

The impurity model is solved using the Continuous-Time Quantum Monte Carlo (CTQMC) in its hybridization expansion (CT-HYB) form^{39,40} implemented by Gull et al⁴¹ in the ALPS package.⁴² We also solved the impurity problem using a Hartree approximation to the interaction. This is the DFT+U approximation, but implemented using the same correlated subspace and double counting as in the DFT+DMFT calculation, enabling an unambiguous comparison of the results obtained from the two methods. In both cases the whole DFT+DMFT loop is iterated until the total energy difference between consecutive updates of charge density is less than 5 meV.

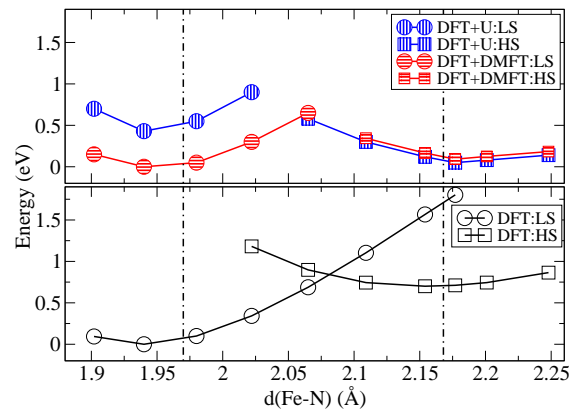


FIG. 1. Dependence of total energy on average Fe-to-N bond length. The DFT+U and DFT+DMFT calculations used $U = U' = 5.0eV$ and $J = 0.85eV$ and the DFT+DMFT calculations were done at 387K. The two dashed lines indicate the experimentally measured average Fe-to-N bond length for LS and HS states.⁴⁴

Spectral functions are obtained via analytic continuation of the computed imaginary time Green's function using the maximum entropy method⁴³ and the Fe contribution to the magnetic susceptibility is calculated from the impurity model spin-spin correlation functions, which are measured in our CTQMC calculations, as

$$\chi_{loc} = (g\mu_B)^2 \int_0^\beta d\tau \langle S_z(0)S_z(\tau) \rangle \quad (2)$$

where S_z is the z component of spin on the impurity site. The total energy (see Refs. 30 and 31 for details) is

$$E^{tot}[\rho, \hat{G}_{loc}] = E^{DFT}[\rho] + E^{KS}[\rho, \hat{G}_{loc}] + E^{pot}[\hat{G}_{loc}] - E^{dc} \quad (3)$$

Here E^{DFT} is the density functional theory approximation to the total energy, $E^{KS}[\rho, \hat{G}_{loc}]$ is a correction to the DFT energy arising from the difference between the DFT and DFT+DMFT density matrices, and the interaction energy term $E^{pot}[\hat{G}_{loc}]$ is calculated from the frequency dependent self-energy $\hat{\Sigma}$ and Green's function as

$$E^{pot} = \frac{1}{2} T \sum_n Tr \left[\hat{\Sigma}(i\omega_n) \hat{G}_{loc}(i\omega_n) \right] \quad (4)$$

To perform structural relaxations within our many-body DFT+DMFT theory, we first define reference structures using structurally relaxed DFT calculations. The metastable HS (LS) state was obtained by using an initialization of the Fe magnetic moment at the nominal high-spin (low-spin) value. We then construct a path between the two structures by linearly interpolating all atomic positions between the values found for the LS and HS structures and minimize the DFT+DMFT energy along this path. We parametrize the path in structure space by the Fe-N bond length.

TABLE I. Energy splitting and optimized average Fe-to-N bond length from DFT, DFT+U and DFT+DMFT calculations.

Method	DFT	DFT+U	DFT+DMFT	Expt ^{21,44}
$E_{HS} - E_{LS}$ (eV)	0.70	-0.38	0.10	0.13
LS $d(Fe - N)$ Å	1.94	1.94	1.94	1.97
HS $d(Fe - N)$ Å	2.15	2.20	2.18	2.17

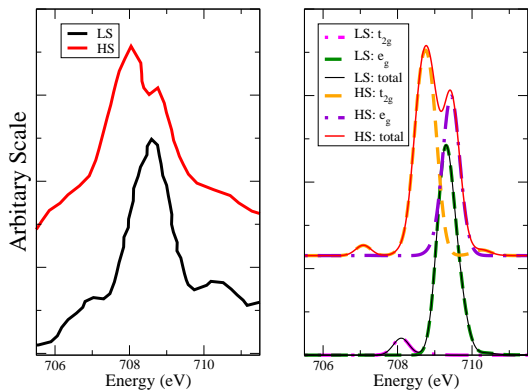


FIG. 2. (a) Fe L_{III} edge X-ray absorption spectroscopy of LS and HS measured at 17K and 298K respectively from Ref. 45. (b) Spectral functions of empty Fe d state from analytic continuation via maximum entropy method. Absolute positions of spectral functions are shifted to match experiment, and dipole matrix elements and core-hole effects were not included in calculations

Fig. 1 shows the structure dependence of the DFT+DMFT energies along with those obtained by density functional and DFT+U methods. All three methods yield two locally stable structures, one with a shorter $d(Fe - N)$, which will be seen to correspond to the LS state, and one with a longer $d(Fe - N)$, which will be seen to be the HS state.

The bond lengths and LS-HS energy splittings computed for the locally stable structures are given in Table I. While all methods give bond lengths in reasonable agreement with experiment, both DFT and DFT+U methods give an inadequate account of the energy differences between the LS and HS structures. DFT predicts that the LS state is much too stable while DFT+U, with a physically reasonable U and J , incorrectly predicts the HS state to be the ground state. Similar to hybrid functional calculations²¹ and previous spin density functional +U calculations,^{25,26} it is possible to tune U to a value that reproduces the observed energy difference within DFT+U, but the required $U \approx 2.5$ eV is unphysically small. By contrast, the DFT+DMFT calculations produce a result in good agreement with experiment with physically reasonable interaction parameters.

The respective electronic states of the short-bond and long-bond structures are found to be locally stable up to the highest temperatures studied $\sim 1200K$; suggesting, in agreement with deductions from experimental data,⁴⁶

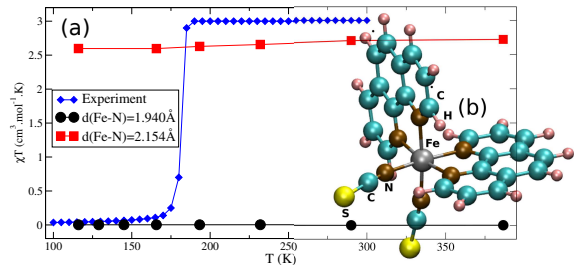


FIG. 3. (a): Temperature dependence of product χT of susceptibility (computed from Eq. 2 with $g = 2$) and temperature from DFT+DMFT calculations for high and low spin structures at $U = 5.0eV$ and $J = 0.85eV$ compared to experimental data.¹²; (b) Molecular structure of $Fe(phen)_2(NCS)_2$

that the electronic entropy and energetics are not enough to drive the observed transition at a fixed bond length. We infer from these results that the Fe-to-N bond length is the critical variable; indeed calculations⁴⁷ show that the LS to HS transition occurs when $d(Fe - N)$ crosses a critical value approximately 2.10\AA . Phonon free energy will determine the actual transition temperature.

From our DFT+DMFT calculations we obtain the many-body density matrix describing the probability of different configurations of the d -orbitals.⁴⁸ We find, as expected, that the dominant configuration in the LS state has zero total spin and is described by an almost complete occupancy of the t_{2g} symmetry d -states. The key issue for the energetics of the LS state is the correct treatment of the virtual charge fluctuations into the e_g states, in light of the strong Coulomb repulsion associated with multiple occupancy of the e_g states. DFT predicts an e_g occupancy of 1.25 electrons and a relatively large hybridization energy gain. Both the e_g occupancy and the hybridization energy gain are likely excessive due to the inadequate treatment of correlations in current DFT implementations. Alternatively, DFT+U, which adds an extra Hartree term, overestimates the correlation energy, providing an e_g occupancy of 0.99 electrons (likely too small) and an underestimate of the hybridization energy. DMFT treats the hybridization more correctly, giving an e_g occupancy of 1.15 and a reasonable value for the energy of the LS state. The improved properties of DFT+DMFT result from a proper characterization of the multiconfigurational character of LS state, as also found in quantum chemistry calculations.⁴⁹ Turning now to the high spin (HS) state, we find that the HS state is found to be the d^5 maximal spin configuration, with only small quantum fluctuations towards d^6 and lower total spin, leading to a mean d -occupancy ~ 5.3 . By neglecting the correlated nature of the virtual hopping into the d^6 configuration DFT+U allows all of the virtual hoppings to add in parallel, thus overestimating the hybridization energy gain, but because the multiconfigurational character of the HS state is weak, the difference between DFT+U

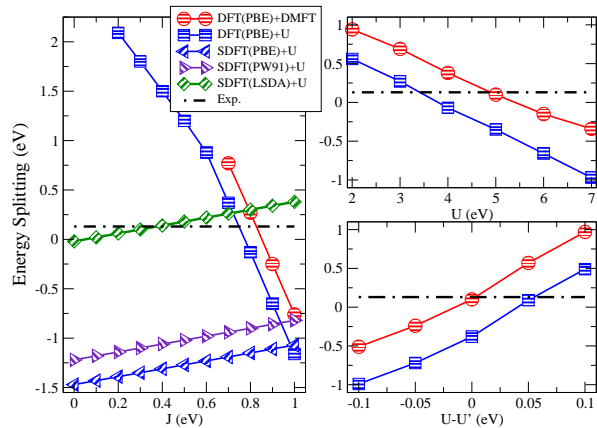


FIG. 4. Left panel: Energy splitting $E_{HS} - E_{LS}$ as function of J for $U = 5eV$. Right upper panel: Energy splitting as function of U for $J = 0.85eV$. Right lower panel: Energy splitting as function of double counting parameter U' (Eq. 5) for $U = 5eV$ and $J = 0.85eV$. Temperature is 387K in DMFT calculations. SDFT+U calculations were performed with projector basis in VASP.

and DFT+DMFT is slight.

Having established accurate energetics, we now turn to spectra and magnetic response. X-ray absorption spectroscopy experiments in which incident X-rays are tuned to the Fe L_{III} edge probe the empty d-states, revealing information about the electronic configuration of the Fe ions. Representative data⁴⁵ are compared to our DFT+DMFT calculations in Fig. 2. The theoretical calculations (right panel) reveal that in the LS configuration the density of empty t_{2g} states is very low; the e_g spectrum reveals a single main peak, with a small prepeak of t_{2g} origin arising from a small probability of a LS d^5 . Alternatively, in the HS situation the two peaks correspond to transitions into the empty t_{2g} and e_g states respectively. The calculated spectra (for example the $t_{2g} - e_g$ crystal field splitting in the HS state) are in reasonably good agreement with the data although not all of the detailed structure away from the main peaks is reproduced (see Ref. 45 for a possible interpretation).

Fig. 3 shows the susceptibility calculated from Eq. 2 along with experimental results from Ref. 12. We see that the structure with long mean Fe-N bond length indeed has a Curie susceptibility $\chi \sim 1/T$ permitting its identification as the HS state, while the short bond (LS) state has a very small susceptibility. Experimental values are $0.5\mu_B$ and $5\mu_B$ for LS and HS, respectively,¹² whereas we obtained around $0.004\mu_B$ for LS and $4.6\sim 4.8\mu_B$ for HS. Our calculations only include the d-electron contribution to χ ; the nearly quantitative agreement with experiment suggests this is the dominant contribution.

Crucial to the DFT+DMFT formalism are the values of the interactions in the correlated subspace and the double counting correction. We have demonstrated a respectable degree of accuracy using the standard double-counting approach and accepted values for the on-site

interactions. However, it is critical to understand the sensitivity of the results to these approximations. The left panel of Fig. 4 shows that the DFT+DMFT and DFT+U results for the LS-HS energy difference depend strongly on J , as expected since J is the term in the energy favoring locally high spin configurations. The magnitude of the slope is sufficiently large that a relatively small increase in the exchange from $J = 0.85eV$ to $J = 0.9eV$ would change the sign of the energy splitting, demonstrating the importance of precisely knowing the exchange. However it is significant that that generally accepted value $J = 0.85eV$ yields an exchange splitting with the correct $\sim 0.1eV$ order of magnitude.

Fig. 4 also shows that three widely used SDFT+U methodologies yield a qualitatively different result as compared to DFT+U (and DFT+DMFT) in two key respects: the magnitude and sign of the slope and the value of the $J = 0$ intercept. The difference in $J = 0$ values of the energy splitting shows that the SDFT have an effective J built in them, due to spin-polarized exchange functional in SDFT; comparison to the J -dependent DFT+U results demonstrates that J_{eff} for SDFT(LSDA)+U, SDFT(PW91)+U, and SDFT(PBE)+U are approximately $J_{eff} \approx 0.75eV$, $J_{eff} \approx 0.93eV$, and $J_{eff} \approx 1.05eV$, respectively. The counterintuitive finding that the SDFT+U energy splitting increases with increasing J can be traced to the spin-dependent double counting correction,

$$V_{dc}^{\sigma} = U(N_d - \frac{1}{2}) - J(\frac{N^{\sigma}}{2} - \frac{1}{2}) \quad (5)$$

which overcompensates the effect of the J in the interaction, increasing the energy splitting. This is a reasonable behavior given that all of the spin-dependent exchange correlation functionals incorrectly predict the energy splitting to be negative at $J = 0$. Therefore, careful analysis is required in the use of SDFT theories as a base on which to build a correlated calculation.

The right upper panel of Fig. 4 presents the U dependence of the HS-LS energy splitting. We see that for each method, a U can be found that reproduces the measured energy difference, and the trends with U are similar in all methods, but the DFT+DMFT method gives the physically correct splitting when a reasonable U is employed. Motivated by previous work on rare earth nickelates,^{30,31} we show in the right lower panel the effects of varying the double counting correction, setting $U' \neq U$ in Eq. 5. For given U , J and U' , the DFT+DMFT procedure always yields a smaller energy difference than the DFT+U methodology. The dependences illustrated in Fig. 4 indicate that in order for the method to become truly predictive, improved theoretical understanding of the interaction parameters and double counting is required. Results presented here can serve as benchmarks for this endeavor.

In summary, we have shown that DFT+DMFT with generally accepted interaction parameters produces energetics, magnetic susceptibilities, and x-ray absorption spectra in reasonable agreement with experimental mea-

surements on $\text{Fe}(\text{phen})_2(\text{NCS})_2$. The method involves a full self-consistency between the correlated subspace and the background, but the locality assumption basic to many solid-state applications of DMFT is here exact because there is only one correlated site. The ability of DFT+DMFT to handle hybridization in a correlated environment is important for the success of the method. The ability to perform calculations for a range of temperatures and structures revealed that electronic energy and entropy considerations do not account for the observed transition. The mean metal-to-ligand bond length

is the key parameter controlling the spin state and the transition is maybe driven by phonon free energy considerations.

The authors would like to thank Hyowon Park for very helpful discussions. This research is supported by U.S. Department of Energy under Grant No. DE-SC0006613. AJM also acknowledges DE-ER046169. We used resources of the National Energy Research Scientific Computing Center, a DOE Office of Science User Facility supported by the Office of Science of the U.S. Department of Energy under Contract No. DE-AC02-05CH11231.

-
- ¹ A. Georges, G. Kotliar, W. Krauth, and M. J. Rozenberg, *Rev. Mod. Phys.* **68**, 13 (1996).
 - ² G. Kotliar, S. Y. Savrasov, K. Haule, V. S. Oudovenko, O. Parcollet, and C. A. Marianetti, *Rev. Mod. Phys.* **78**, 865 (2006).
 - ³ S. Florens, *Phys. Rev. Lett.* **99**, 046402 (2007).
 - ⁴ A. Valli, O. Sangiovanni, O. Gunnarsson, A. Toschi, and K. Held, *Phys. Rev. Lett.* **104**, 246402 (2010).
 - ⁵ D. Jakob, K. Haule, and G. Kotliar, *Phys. Rev. B* **82**, 195115 (2010).
 - ⁶ V. Turkowski, A. Kabir, N. Nayyar, and T. Rahman, *J. Phys. Cond. Matt.* **22**, 462202 (2010).
 - ⁷ N. Lin, C. A. Marianetti, A. J. Millis, and D. R. Reichman, *Phys. Rev. Lett.* **106**, 096402 (2011).
 - ⁸ D. Zgid and G. K.-L. Chan, *The Journal of Chemical Physics* **134**, 094115 (2011).
 - ⁹ A. Kabir, V. Turkowski, and T. Rahman, arXiv **1311.3147** (2013).
 - ¹⁰ C. Weber, D. J. Cole, D. D. O'Regan, and M. C. Payne, *Proceedings of the National Academy of Sciences* **111**, 5790 (2014).
 - ¹¹ C. Weber, D. D. O'Regan, N. D. M. Hine, P. B. Littlewood, G. Kotliar, and M. C. Payne, *Phys. Rev. Lett.* **110**, 106402 (2013).
 - ¹² S. Shi, G. Schmerber, J. Arabski, J.-B. Beaufrand, D. J. Kim, S. Boukari, M. Bowen, N. T. Kemp, N. Viart, G. Rogez, E. Beaurepaire, H. Aubriet, J. Petersen, C. Becker, and D. Ruch, *Applied Physics Letters* **95**, 043303 (2009).
 - ¹³ X. Zhang, T. Palamarciuc, J.-F. Letard, P. Rosa, E. V. Lozada, F. Torres, L. G. Rosa, B. Doudin, and P. A. Dowben, *Chem. Commun.* **50**, 2255 (2014).
 - ¹⁴ T. Miyamachi, M. Gruber, V. Davesne, M. Bowen, S. Boukari, L. Joly, F. Scheurer, G. Rogez, T. K. Yamada, P. Ohresser, E. Beaurepaire, and W. Wulfhekkel, *Nat Commun* **3**, 938 (2012).
 - ¹⁵ E. König and K. Madeja, *Chem. Commun.* **0**, 61 (1966).
 - ¹⁶ P. Gütllich, A. Hauser, and H. Spiering, *Angewandte Chemie International Edition in English* **33**, 2024 (1994).
 - ¹⁷ P. Gütllich, Y. Garcia, and H. A. Goodwin, *Chem. Soc. Rev.* **29**, 419 (2000).
 - ¹⁸ V. I. Anisimov, J. Zaanen, and O. K. Andersen, *Phys. Rev. B* **44**, 943 (1991).
 - ¹⁹ V. I. Anisimov, I. V. Solovyev, M. A. Korotin, M. T. Czyżyk, and G. A. Sawatzky, *Phys. Rev. B* **48**, 16929 (1993).
 - ²⁰ B. Gallois, J. A. Real, C. Hauw, and J. Zarembowitch, *Inorganic Chemistry* **29**, 1152 (1990).
 - ²¹ M. Reiher, *Inorganic Chemistry* **41**, 6928 (2002).
 - ²² A. Slimani, X. Yu, A. Muraoka, K. Boukheddaden, and K. Yamashita, *The Journal of Physical Chemistry A* **118**, 9005 (2014).
 - ²³ S. Ye and F. Neese, *Inorganic Chemistry* **49**, 772 (2010).
 - ²⁴ S. L. Dudarev, G. A. Botton, S. Y. Savrasov, C. J. Humphreys, and A. P. Sutton, *Phys. Rev. B* **57**, 1505 (1998).
 - ²⁵ S. Lebegue, S. Pillet, and J. G. Ángyán, *Phys. Rev. B* **78**, 024433 (2008).
 - ²⁶ T. Bucko, J. Hafner, S. Lebegue, and J. G. Angyan, *Phys. Chem. Chem. Phys.* **14**, 5389 (2012).
 - ²⁷ A. Droghetti, D. Alfè, and S. Sanvito, *The Journal of Chemical Physics* **137**, 124303 (2012).
 - ²⁸ A. Droghetti, D. Alfè, and S. Sanvito, *Phys. Rev. B* **87**, 205114 (2013).
 - ²⁹ A. Rudavskiy, C. Sousa, C. de Graaf, R. W. A. Havenith, and R. Broer, *The Journal of Chemical Physics* **140**, 184318 (2014).
 - ³⁰ H. Park, A. J. Millis, and C. A. Marianetti, *Phys. Rev. B* **89**, 245133 (2014).
 - ³¹ H. Park, A. J. Millis, and C. A. Marianetti, *Phys. Rev. B* **90**, 235103 (2014).
 - ³² G. Kresse and J. Furthmüller, *Phys. Rev. B* **54**, 11169 (1996).
 - ³³ G. Kresse and D. Joubert, *Phys. Rev. B* **59**, 1758 (1999).
 - ³⁴ J. P. Perdew, K. Burke, and M. Ernzerhof, *Phys. Rev. Lett.* **77**, 3865 (1996).
 - ³⁵ A. A. Mostofi, J. R. Yates, Y.-S. Lee, I. Souza, D. Vanderbilt, and N. Marzari, *Computer Physics Communications* **178**, 685 (2008).
 - ³⁶ E. Pavarini, "The lda+dmft approach to strongly correlated materials: lecture notes of the autumn school 2011," (Forschungszentrum, Zentralbibliothek Jülich, 2011) Chap. The LDA+DMFT Approach.
 - ³⁷ A. Kutepov, K. Haule, S. Y. Savrasov, and G. Kotliar, *Phys. Rev. B* **82**, 045105 (2010).
 - ³⁸ Z. P. Yin, K. Haule, and G. Kotliar, *Nat Phys* **7**, 294 (2011).
 - ³⁹ P. Werner, A. Comanac, L. de' Medici, M. Troyer, and A. J. Millis, *Phys. Rev. Lett.* **97**, 076405 (2006).
 - ⁴⁰ E. Gull, A. J. Millis, A. I. Lichtenstein, A. N. Rubtsov, M. Troyer, and P. Werner, *Rev. Mod. Phys.* **83**, 349 (2011).
 - ⁴¹ H. Hafermann, P. Werner, and E. Gull, *Computer Physics Communications* **184**, 1280 (2013).
 - ⁴² B. Bauer, L. D. Carr, H. G. Evertz, A. Feiguin, J. Freire,

- S. Fuchs, L. Gamper, J. Gukelberger, E. Gull, S. Guertler, A. Hehn, R. Igarashi, S. V. Isakov, D. Koop, P. N. Ma, P. Mates, H. Matsuo, O. Parcollet, G. Pawowski, J. D. Picon, L. Pollet, E. Santos, V. W. Scarola, U. Schollwck, C. Silva, B. Surer, S. Todo, S. Trebst, M. Troyer, M. L. Wall, P. Werner, and S. Wessel, *Journal of Statistical Mechanics: Theory and Experiment* **2011**, P05001 (2011).
- ⁴³ M. Jarrell and J. Gubernatis, *Physics Reports* **269**, 133 (1996).
- ⁴⁴ V. Legrand, S. Pillet, H.-P. Weber, M. Souhassou, J.-F. Létard, P. Guionneau, and C. Lecomte, *Journal of Applied Crystallography* **40**, 1076 (2007).
- ⁴⁵ J.-J. Lee, H.-s. Sheu, C.-R. Lee, J.-M. Chen, J.-F. Lee, C.-C. Wang, C.-H. Huang, and Y. Wang, *Journal of the American Chemical Society* **122**, 5742 (2000).
- ⁴⁶ M. Sorai and S. Seki, *Journal of Physics and Chemistry of Solids* **35**, 555 (1974).
- ⁴⁷ See Supplemental Material at [URL will be inserted by publisher] for the dependence of magnetic susceptibility on temperature and $d(Fe - N)$.
- ⁴⁸ See Supplemental Material at [URL will be inserted by publisher] for various characterizations of d-orbitals configurations.
- ⁴⁹ A. Domingo, M. Ángels Carvajal, and C. de Graaf, *International Journal of Quantum Chemistry* **110**, 331 (2010).
- ⁵⁰ V. Křápek, P. Novák, J. Kuneš, D. Novoselov, D. M. Krotin, and V. I. Anisimov, *Phys. Rev. B* **86**, 195104 (2012).
- ⁵¹ P. Augustinský, V. Křápek, and J. Kuneš, *Phys. Rev. Lett.* **110**, 267204 (2013).
- ⁵² N. Marzari, A. A. Mostofi, J. R. Yates, I. Souza, and D. Vanderbilt, *Rev. Mod. Phys.* **84**, 1419 (2012).
- ⁵³ H. Park, A. J. Millis, and C. A. Marianetti, *Phys. Rev. Lett.* **109**, 156402 (2012).
- ⁵⁴ E. Miller, H. Spiering, and P. Gtlich, *Chemical Physics Letters* **93**, 567 (1982).
- ⁵⁵ A. I. Liechtenstein, V. I. Anisimov, and J. Zaanen, *Phys. Rev. B* **52**, R5467 (1995).
- ⁵⁶ K. Haule, *Physical Review B (Condensed Matter and Materials Physics)* **75**, 155113 (2007).
- ⁵⁷ X. Wang, M. J. Han, L. de' Medici, H. Park, C. A. Marianetti, and A. J. Millis, *Phys. Rev. B* **86**, 195136 (2012).
- ⁵⁸ H. T. Dang, A. J. Millis, and C. A. Marianetti, *Phys. Rev. B* **B89**, 161113 (2014).
- ⁵⁹ H. T. Dang, X. Ai, A. J. Millis, and C. A. Marianetti, *Phys. Rev. B* **B90**, 125114 (2014).
- ⁶⁰ T. Helgaker, P. Jørgensen, and J. Olsen, *Molecular Electronic-Structure Theory* (John Wiley and Sons, Ltd, Baffins Lane, Chichester, West Sussex PO19 IUD, England, 2000).
- ⁶¹ N. Parragh, G. Sangiovanni, P. Hansmann, S. Hummel, K. Held, and A. Toschi, *Phys. Rev. B* **88**, 195116 (2013).
- ⁶² O. E. Peil, M. Ferrero, and A. Georges, *Phys. Rev. B* **90**, 045128 (2014).